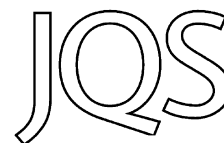


Mid-elevation ecosystems of Panama: future uncertainties in light of past global climatic variability



ALEXANDER CORREA-METRIO,^{1*} MARIA I. VÉLEZ,² JAIME ESCOBAR,^{3,4}
JEANNINE-MARIE ST-JACQUES,⁵ MINERVA LÓPEZ-PÉREZ,⁶ JASON CURTIS⁷ and JASON COSFORD²

¹Instituto de Geología, Universidad Nacional Autónoma de México, Coyoacán, México D.F. 04510, México

²Department of Geology, University of Regina, Regina, Saskatchewan, S4S 7H9, Canada

³Departamento de Ingeniería Civil y Ambiental, Universidad del Norte, Barranquilla, Colombia

⁴Center for Tropical Paleocology and Archaeology, Smithsonian Tropical Research Institute, Balboa-Ancon, Box 0843-03092, Panama

⁵Prairie Adaptation Research Collaborative, University of Regina, Regina, Saskatchewan, S4S 0A2, Canada

⁶Posgrado en Ciencias Biológicas, Universidad Nacional Autónoma de México, Coyoacán, México D.F. 04510, México

⁷Department of Geological Sciences, University of Florida, Gainesville, FL 32611, USA

Received 26 December 2015; Revised 1 July 2016; Accepted 24 August 2016

ABSTRACT: Modern changes in regional climates will result in high ecosystem turnover and substantial biodiversity rearrangements. Understanding these changes requires palaeoecological studies at temporal resolutions comparable to the time window at which modern climate change is occurring. Here we present a multi-proxy, high-resolution record of forest and lake ecosystem change that occurred during the last 1100 years at middle elevations in Panama. From ~900 to 1400 CE, regional forest and lake ecosystems were characterized by high seasonality, probably associated with both high El Niño activity and higher global temperatures. At ~1400 CE, an abrupt transition marked the decoupling of forest and lake responses, with forest responding mostly to local patterns of human occupation, and lake trophic status being controlled mostly by the regional precipitation–evaporation balance, possibly associated with solar irradiance. Factors that played important roles in shaping regional ecosystems during the last 1100 years will probably again play critical roles within the coming decades, i.e. higher precipitation seasonality and higher temperatures. Past responses of the system, together with pervasive human activities, suggest that future conditions will simplify mid-elevation forests. Given the importance of these geographical locations as hotspots of biological diversity, substantial losses of global biodiversity are foreseen. Copyright © 2016 John Wiley & Sons, Ltd.

KEYWORDS: biodiversity; climate change; Little Ice Age; Medieval Climate Anomaly; precipitation seasonality.

Introduction

Multi-annual climate variability plays a fundamental role in shaping vegetation assemblages and influencing aquatic ecosystems. Indeed, modern displacement of climate space occurring at decadal time scales will probably result in high ecosystem turnover and substantial biodiversity rearrangements (Loarie *et al.*, 2009). In past times, the amount of extraterrestrial energy received by Earth has exerted strong control on climate and ecosystems at millennial to sub-millennial time scales (Bush and Colinvaux, 1990; Hodell *et al.*, 2001). Over shorter time scales, regional patterns of climate variability, and therefore the evolution of ecosystems, are mostly modulated by the planet's intrinsic dynamics, e.g. the El Niño–Southern Oscillation (Moy *et al.*, 2002; Conroy *et al.*, 2008; Toth *et al.*, 2015). Thus, palaeoclimatic and palaeoecological studies are useful to understand the effects of modern climate changes on ecosystem structure and function in the future. Such is the case of abrupt climate change, defined by the IPCC Fifth Assessment Report as a large-scale change in the climate system that takes place over a few decades or less and persists long enough to cause disruptions in human and natural systems (IPCC, 2013). However, understanding this requires decadal-to-subcentennial temporal-scale records that allow the evaluation of biotic systems' sensitivity to global changes similar to those taking place today.

The geological and climatic histories of Panama have favoured the development of exceptionally rich biodiversity. Whereas the closure of the Panama Isthmus facilitated the

convergence of elements from the Nearctic and Neotropical floras and faunas (Graham, 2010), Quaternary climatic variability has modulated the resultant biodiversity at different time scales (e.g. Bush and Colinvaux, 1990; Bush *et al.*, 1992). High diversity has been maintained through time by migration, adaptation and the existence of microrefugia (Bush, 2002; Correa-Metrio *et al.*, 2014). These ecological features are of particular interest in the middle elevations of the tropical mountain ranges (premontane and lower montane altitudinal belts of Holdridge *et al.*, 1964), regions that have been poorly studied in terms of their environmental history. These areas are characterized by broad environmental gradients over relatively short distances, and high topographic diversity that makes highly likely the existence of microhabitats that could be used as refugia during times of environmental hardship (Bush, 2002). Thus, palaeoecological studies from these regions would contribute to understanding the role of the middle elevations at sheltering diversity through time.

Here we present a 20-year resolution environmental reconstruction that spans the last ~1100 years. It is based on multiple proxies from a sediment core collected from Lake San Carlos, an 8.3-m-deep water body that occupies 3 ha at 783 m a.s.l. in central Panama (Fig. 1). We analysed pollen, charcoal, diatoms and organic carbon isotopes to infer vegetation and lake dynamics through time. Given the lake's geographical location, the time span covered by the sediment core, and the temporal resolution we used for our analyses, the record offers a unique opportunity to study the interplay between local and global environmental drivers at different time scales. In fact, we provide hints on the confluence of global temperature

*Correspondence to: A. Correa-Metrio, as above.
E-mail: acorrea@geologia.unam.mx

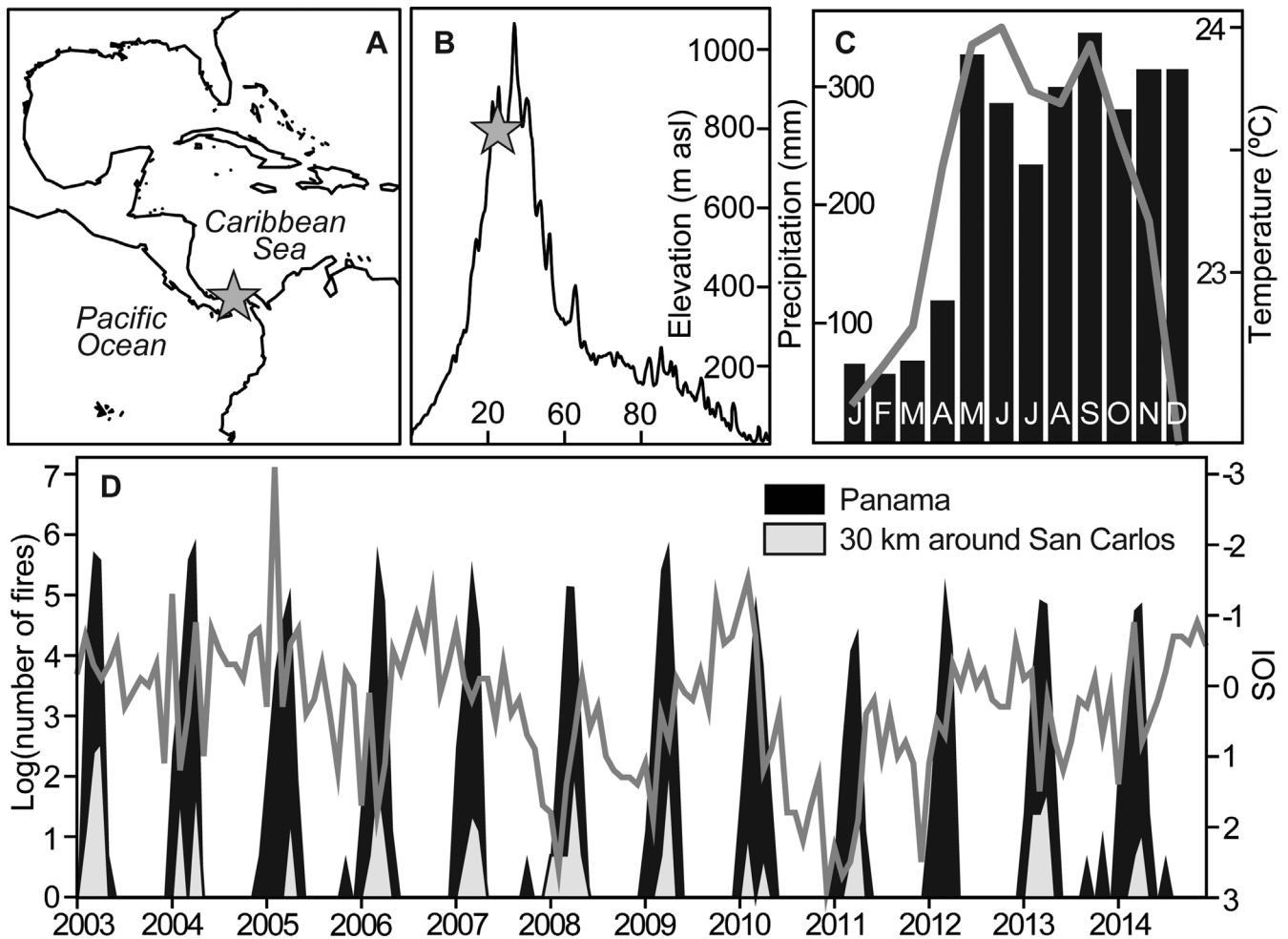


Figure 1. Study area. (A) Location of Lake San Carlos on the Panama Isthmus. (B) Elevation profile of the Central Cordillera of Panama showing the location of Lake San Carlos; the x-axis is distance measured in kilometres from the Pacific Ocean to the Caribbean Sea, and the y-axis is elevation (m a.s.l.). (C) Climograph from the meteorological station at Jagua, 14 km north of Lake San Carlos; precipitation, bars; temperature, grey line. (D) Monthly number of fires (logarithmic scale) in Panama (black) and San Carlos (solid grey) and the Southern Oscillation Index (SOI, grey line) from January 2003 to December 2014; tick marks represent January of each year. Cross-correlation between the SOI and the total number of fires in Panama (fire data from NASA FIRMS, Giglio *et al.*, 2003) resulted in significant correlations at lags of between 2 and 7 months, and range between -0.22 and -0.17 . Sustained negative values of the SOI indicate development of El Niño activity in the Pacific, which causes drier than normal conditions in Panama, and therefore higher fire activity.

changes that occurred during the Medieval Climate Anomaly warming (MCA) and the Little Ice Age cooling (LIA) (Mann *et al.*, 2009), and regional and local factors such as El Niño frequency (Moy *et al.*, 2002; Conroy *et al.*, 2008), and human occupation that has been documented for the area throughout the Holocene (e.g. Cooke, 2005; Piperno, 2006).

Study area

Lake San Carlos is a small (~ 3.3 ha), shallow ($z_{\max} = \sim 8.3$ m), hydrologically closed water body located in central Panama ($8^{\circ}37'32.44''\text{N}$, $80^{\circ}03'4.24''$, 783 m a.s.l.). The lake lies on a volcanic substrate on the Pacific flank of the Central Cordillera of Panama (Fig. 1). At an elevation of ~ 780 m a.s.l., the northern and eastern shores of the lake abut cliffs that reach up to 1000 m a.s.l. (Supporting Information, Appendix S1). In contrast, the western and southern shores give way to slopes that descend towards the Gulf of Panama coastline, about 18 km away. With a mean annual precipitation of 2700 mm, 190 mm falling during the driest quarter, the regional vegetation of San Carlos represents the transition between wet and seasonal moist forest (Graham, 2010; Leigh *et al.*, 2014). Most of the precipitation of the Pacific flank of the Central Cordillera comes from the Pacific Ocean that leads to a seasonal pattern in its intra-annual distribution.

Because of the elevation, moisture deficit through the dry quarter is ameliorated by lower evaporation and orographic precipitation. Additionally, the areas of the Central Cordillera that are near the mountain ridge that divides the Pacific and Caribbean flanks probably receive moisture subsidies from the Caribbean Sea. Thus, the Lake San Carlos basin would be highly sensitive to climate changes at sub-centennial time scales (e.g. changes in the atmospheric convective activity over the ocean and seasonal distribution of temperature).

Methods

In 2012, a 276-cm-long sediment core was retrieved from Lake San Carlos, central Panama, using a Livingstone piston corer (Colinvaux *et al.*, 1999). Chronological control for the record was established using five radiocarbon dates at different depths (Appendix S2). These radiocarbon dates were calibrated using the IntCal13 curve (Reimer *et al.*, 2013) and used to construct a Bayesian depth–age model using Bacon (Blaauw and Christen, 2011).

The core was sampled every 5 cm for diatoms, pollen and charcoal analyses, which were undertaken using standard techniques. For diatom analyses, 0.2 g of dry sediment from each depth was digested in 30 mL H_2O_2 for 48 h, and two 0.3-mL aliquots were mounted on microscope slides

(Battarbee *et al.*, 2001). Diatoms in each sample were counted until at least 400 diatom frustules were enumerated. For pollen analysis, 0.5 cm³ of sediment from each depth was deflocculated and prepared using standard protocols (Faegri and Iversen, 1989), which included acetolysis and gravimetric separation. Pollen grains in each sample were counted until a sum of 300 pollen grains was reached, excluding spores and aquatics. For charcoal analysis, 0.5-cm³ samples of wet sediment were deflocculated using sodium pyrophosphate, and charcoal particles were manually separated under a stereomicroscope (Clark, 1988). Photographs of all particles were taken to estimate their area and calculate charcoal concentration (mm² cm⁻³). Relative abundances of pollen and diatoms are expressed as percentages of the total sum in each sample, and charcoal is expressed as area per volume (mm² cm⁻³).

The core was sampled every 2 cm for organic carbon isotopic analyses. Sediment samples were freeze-dried and crushed with a mortar and pestle. Approximately 3–15 µg of carbonate-free bulk sediment was loaded into tin sample capsules placed in a 50-position automated carousel on a Carlo Erba NA 1500 elemental analyser. After combustion in a quartz column at 1020 °C in an oxygen-rich atmosphere, the sample gas was transported in an He carrier stream and passed through a hot reduction column (650 °C) consisting of elemental copper to remove oxygen. The effluent stream then passed through a chemical (magnesium perchlorate) trap to remove water followed by a 0.8-m GC column at 115 °C to separate N₂ from CO₂. The sample gas next passed into a Conflo II preparation system and into the inlet of a Thermo Electron Delta V Advantage isotope ratio mass spectrometer running in continuous flow mode where the sample gas was measured relative to laboratory reference N₂ and CO₂ gases. The isotopic analyses included 26 measurements of USG40 standard that yielded a standard deviation of 0.03‰ for carbon isotopes. Organic carbon isotopes are expressed in standard delta notation relative to VPDB ($\delta^{13}\text{C}_{\text{org}}$ hereafter).

All data were plotted in stratigraphic diagrams using C2 (Juggins, 2007). A principal-component analysis (PCA) was performed using all data to identify and summarize environmental variability through time. Whereas isotopic data were used untransformed, pollen, diatom and charcoal data were log transformed to meet the multi-normality assumption of the PCA (Legendre and Legendre, 1998). Additionally, variables were standardized to take them to common units, avoiding spurious effects of dimensional heterogeneity (i.e. natural units of isotopic data with logarithmic units of biological data). The temporal structure of sample scores in PCA axes 1 and 2 was analysed through moving, non-parametric probability density functions (Silverman, 1986). For this, time windows of 200 years were analysed through non-parametric probability density functions to identify the 95% confidence intervals of environmental variability. Thus, this analysis provides an approximation to the centennial environmental variability, summarizing for each time point PCA scores within a 200-year temporal context. All statistical analyses were performed using R (R Core Team, 2015).

Results

The sedimentary sequence from Lake San Carlos was mostly composed of organic clay and peat with a layer characterized by clay/peat fine laminae between ~145 and 125 cm below lake floor (Fig. 2). With a basal age of ~1080 cal a BP (870 CE) at a depth of 276 cm below lake floor, the average sedimentation rate over the whole core was ~0.24 cm a⁻¹. Although all dates were in stratigraphic order, the upper three

dates were statistically undifferentiable (Fig. 2; Appendix S2). These three dates could be representing a layer of sediments produced by a rapid or even instantaneous deposition event. However, the three dates came from layers of sediment of distinctive nature (Fig. 2), suggesting they were deposited at different times. Their lack of statistical difference might be the result of recurrent ¹⁴C ages during the most recent centuries in the IntCal13 calibration curve (Appendix S2, Reimer *et al.*, 2013). The probability distribution of calibrated ages for each of these three ¹⁴C dates coincided around three time points (~1790, 1650 and 1540 CE, Appendix S2), and we selected the highest probability peak from each of them to produce the most parsimonious age model (Fig. 2; Appendix S2).

Our results show a highly dynamic pattern of environmental changes (Figs. 3 and 4; Appendices S3 and S4). The most important change in regional vegetation occurred around 1400 CE, when the dominance of Asteraceae, Areacaceae, *Bursera* and Poaceae was replaced by *Anacardium*, *Cordia*, Moraceae, *Spondias* and *Zanthoxylum*, among others (Fig. 3). Also, an important change took place at ~1150 CE, when pollen taxa such as *Begonia*, *Eugenia*, *Cespedezia*, Melastomataceae and *Trichilia* became abundant and persisted up to the present (Fig. 3). *Zea mays* (maize) was represented from ~1550 CE to the present, accompanied by a slight increasing trend in *Cecropia*, *Celtis*, Poaceae and Asteraceae, and decreases in Moraceae. Stable carbon isotopes on organic matter followed the trend shown by Poaceae and Asteraceae (Fig. 4). High values of $\delta^{13}\text{C}_{\text{org}}$ characterized the sediments from the bottom of the record to ~1400 CE (average -25.25‰, Fig. 4). At ~1400 CE, $\delta^{13}\text{C}_{\text{org}}$ reached an absolute minimum (-31.13‰), followed by an increasing trend that reached relatively stable values between 1830 CE and the present (-24.73‰, Fig. 4). Similarly, high charcoal concentrations characterized the period between the bottom of the record and 1400 CE, when a decreasing trend started and reached values near zero from ~1700 to the present (Fig. 4).

The diatom record was heavily dominated by *Fragilaria crotonensis*, although peaks in other species differentiated three main assemblages. From the bottom of the record up to ~1150 CE, *F. crotonensis* showed relatively low percentages and was mostly accompanied by *Aulacoseira granulata* var. *angustissima*, *Diademsis contenta*, *Encyonema silesiacum*, *Eunotia formica*, *Navicula lanceolata*, *N. leptostriata* and *N. radiosa* (Fig. 3). From ~1150 to ~1700 CE, the diatom assemblages were almost entirely dominated by *F. crotonensis* with occasional peaks of other species. From ~1700 CE to the present, there was a decreasing trend in the abundance of *F. crotonensis*, and relatively high percentages of *Achnanthes minutissimum*, *A. exiguum*, *Discostella stelligera*, *E. silesiacum* and *Nitzschia amphibia* (Fig. 3).

The first two axes of the PCA explained 84.7% of the total variance contained in the dataset (Axis 1, 81.8%; Axis 2, 2.9%). However, when variables were standardized before the analysis, the percentage of explained variance went down to 21% (Axis 1, 12.16%; Axis 2, 8.74%), with axes above the 5th dimension associated with <5% of the variance. Vectors associated with pollen taxa mostly aligned with PCA Axis 1, and vectors associated with diatoms aligned with PCA Axis 2 (Fig. 5). PCA Axis 1 sample scores were high from the bottom of the record to ~1350 CE, showing a transition to low values, which in turn prevailed from ~1400 to ~1650 CE. From ~1700 CE to the present, sample scores were intermediate (Fig. 6). In contrast, PCA Axis 2 sample scores were low and variable from the bottom of the record to 1700 CE, but trended towards higher values thereafter.

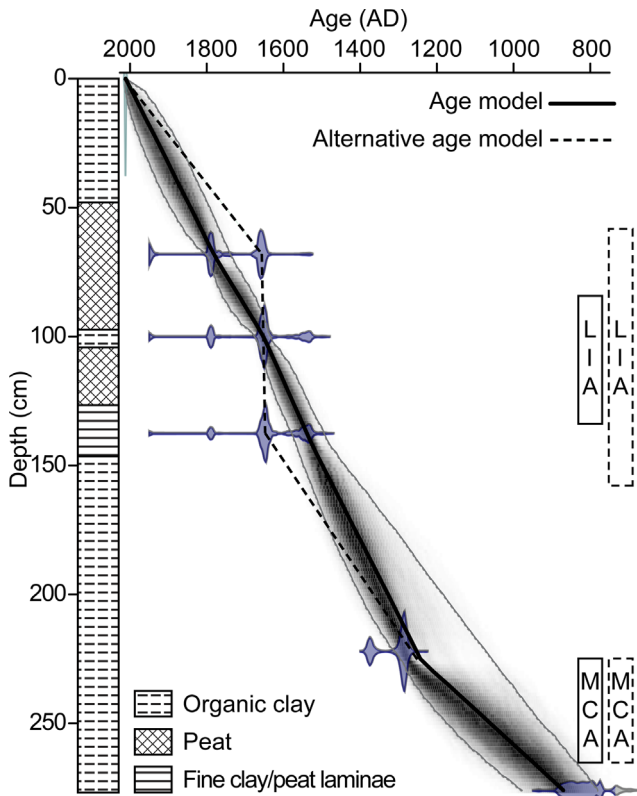


Figure 2. Basic stratigraphy and age–depth model of the sedimentary deposit of Lake San Carlos. The right rectangles show the depth intervals for the Medieval Climate Anomaly and the Little Ice Age under the constructed age model (solid lines) and an alternative model that considers the upper radiocarbon dates as equal (dashed lines).

Discussion

Environments of middle-elevation central Panama through the last millennium

Pollen, diatom, charcoal and stable isotope data show a dynamic pattern of vegetation and lake trophic state changes in middle-elevation central Panama over the last ~1100 years. The raw data and PCA ordination scores (Figs. 3, 4 and 6) indicate at least five different environmental settings through the last millennium. This discretization is not meant to create a formal biostratigraphy, but rather to facilitate the description and interpretation of the regional environmental history.

From ~950 to ~1150 CE, the vegetation was dominated by weeds (Asteraceae) and grasses (Poaceae), which together with high abundances of *Bursera* and palms (Arecaceae) suggest dominance of low-stature vegetation (Figs. 3 and 4). Through the studied period, $\delta^{13}C_{org}$ mostly remained within the range that has been reported for C3 plants (between ~-32 and -24‰, Meyers, 2003), indicating there has not been a significant change in the main primary productivity sources. Nevertheless, from the bottom of the record to ~1400 CE, the dominance of grass pollen might have been the cause of the relatively high $\delta^{13}C_{org}$ values. In the middle and low elevations of Panama and Costa Rica, the only modern pollen spectra with similar percentages of open vegetation elements come from savannas (Rodgers and Horn, 1996; Bush, 2000). However, the isotopic evidence does not support the interpretation of this vegetation type dominating the landscape. Pollen spectra that characterized this period have also been observed in modern samples from seasonal forests on the Yucatán Peninsula (Correa-Metrio *et al.*, 2011). According to our data, this is a more likely scenario for our

study area, which was probably occupied by a highly seasonal tropical forest with recurrent fires (high charcoal concentrations) maintaining relatively open vegetation throughout this period (Fig. 4). It is likely that human occupation, which has been documented archaeologically in the region from the middle to late Holocene (Cooke, 2005; Piperno, 2006), also played a role in maintaining the low-stature forest. In fact, the connection between more seasonal climates and human occupation is evident in multiple records from Central and South America (Piperno *et al.*, 2015). The *Z. mays* record in the San Carlos core, however, indicates that the most intense human activities occurred from 1500 CE to the present (Fig. 4), i.e. after European arrival, and during a period of less precipitation seasonality. High abundances of diatom taxa such as *Achnanthisdium* spp., *Aulacoseira* spp., *D. contenta*, *E. formica*, *E. silesiacum* and *Navicula* spp. during this period (Fig. 3) suggest mesotrophic to eutrophic conditions in the lake (Bellinger *et al.*, 2006). The high trophic state of the lake during this period was probably influenced by the open nature of the vegetation, in that (i) there was more nutrient delivery associated with high rates of terrigenous erosion, and (ii) the lack of dense forest around the lake led to frequent wind-mixing of the water column.

From ~1150 to 1400 CE, high charcoal concentrations and relatively high $\delta^{13}C_{org}$ values (Fig. 4) suggest that seasonal conditions were still dominant. Nevertheless, increasing relative abundances of moist forest taxa such as *Alchornea*, *Begonia*, *Eugenia* and *Trichillia* (Marchant *et al.*, 2002) indicate a trend towards higher precipitation and less seasonality. Increases in relative abundances of pioneer taxa such as *Cecropia* and *Cespedezia*, and high variability of Poaceae and Moraceae (Fig. 3), suggest that environmental conditions were dominated by the transition from dry to moist tropical forest. *Fragilaria crotonensis*, a planktonic diatom species that is highly competitive under low-light conditions (Bradbury, 1988), began to dominate the diatom assemblages, with percentages up to 90% (Fig. 3). It is likely that the development of a dense tree canopy projected afternoon shade onto the relatively small lake, which has always been sheltered from morning sunlight by the cliffs that characterize its north-eastern edge.

Evidence from speleothems and corals suggests the prevalence of dry and warm conditions in central Panama between ~950 and 1400 CE (Lachniet *et al.*, 2004; Toth *et al.*, 2015). Accordingly, our pollen data for this period suggest dry and seasonal conditions, divided into two climate stages. Between ~950 and ~1150 CE, the pollen spectra are very similar to modern assemblages from the Yucatán Peninsula at locations that receive annual rainfall of ~1400 mm (Correa-Metrio *et al.*, 2011). This suggests that during the MCA (950–1250 CE), annual precipitation in the middle elevations of Panama fell to half the modern value, representing the driest period of the last two millennia, and being consistent with reported regional and continental droughts (Hodell *et al.*, 2001; Lachniet *et al.*, 2004). Between ~1150 and ~1400 CE, progressive increases in tropical rainforest (TRF) taxa and decreases in $\delta^{13}C_{org}$ suggest a trend towards wetter conditions, probably reaching modern precipitation values (2700 mm a⁻¹, Fig. 1) by the end of this period.

From ~1400 to 1550 CE, the establishment of dense TRF is shown by the highest relative pollen abundances of taxa such as *Anacardium*, *Cordia*, Moraceae, *Spondias* and *Zanthoxylum* (Fig. 3). A concomitant decrease in charcoal concentrations and the lowest $\delta^{13}C_{org}$ values of the record further support the inference of a dense TRF occupying the area (Fig. 4). The end of this period was marked by the first appearance of maize pollen, indicating human occupation

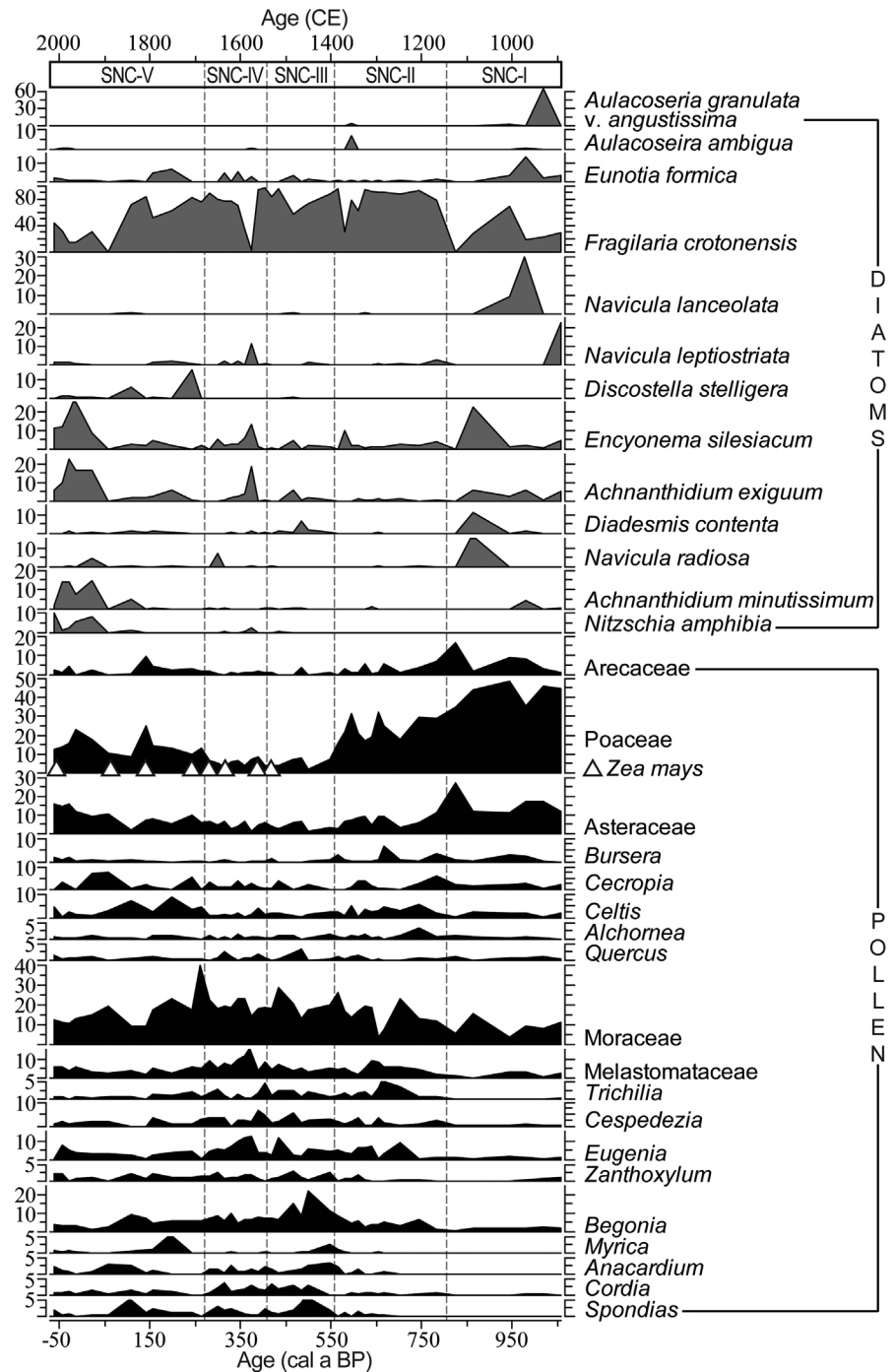


Figure 3. Selected diatom and pollen records from Lake San Carlos sediment core.

near the lake. Subsequently, from 1550 to 1700 CE, there was an increase of ~10% in lower montane forest (LMF) taxa, mainly Melastomataceae and *Quercus*, whereas the abundance of TRF taxa remained relatively stable. This vegetation mixture suggests that whereas minimum temperature remained unchanged, maximum temperature, which represents the limiting factor for montane vegetation, decreased. Mean annual temperature decreases with altitude at an average rate of $6\text{ }^{\circ}\text{C km}^{-1}$, a temperature gradient known as lapse rate (Graham, 2010). Modern LMF in Panama has its lower altitudinal boundary at ~1100m a.s.l. (Brujinzeel, 2001), implying that under the mentioned lapse rate, the highest temperature of the year at Lake San Carlos (~780m a.s.l.) during the LIA was ~1.8 °C lower than today. The increase in LMF taxa coincided with increased ice accumulation on the Quelccaya ice cap in Peru (Thompson *et al.*, 2013) (Fig. 3), indicating that the cooling revealed by our record was probably associated with the first half of the LIA, the coldest

period of the last several millennia (Mann *et al.*, 2009). The LIA has been reported as a dry period for several locations in the Neotropics (e.g. Haug *et al.*, 2003; Hodel *et al.*, 2005; Novello *et al.*, 2012); the San Carlos record shows no sign of drier conditions at that time. Relatively high charcoal concentrations were probably the result of local human activities, revealed by the presence of maize pollen (Fig. 4).

Moist aseasonal conditions between 1530 and 1670 CE were probably the result of lower temperatures, which resulted in less evaporation. Also, the persistence of orographic precipitation on the flanks of the mountains, as has been reported for other locations (Lozano-García *et al.*, 2007), could have offset any regional precipitation decrease. These two factors probably maintained a low soil moisture deficit, so there was no substantial change in vegetation structure. A change in composition is nevertheless evident, with local flora relatively enriched by downslope migration of LMF taxa, a pattern that probably occurred regionally. Our

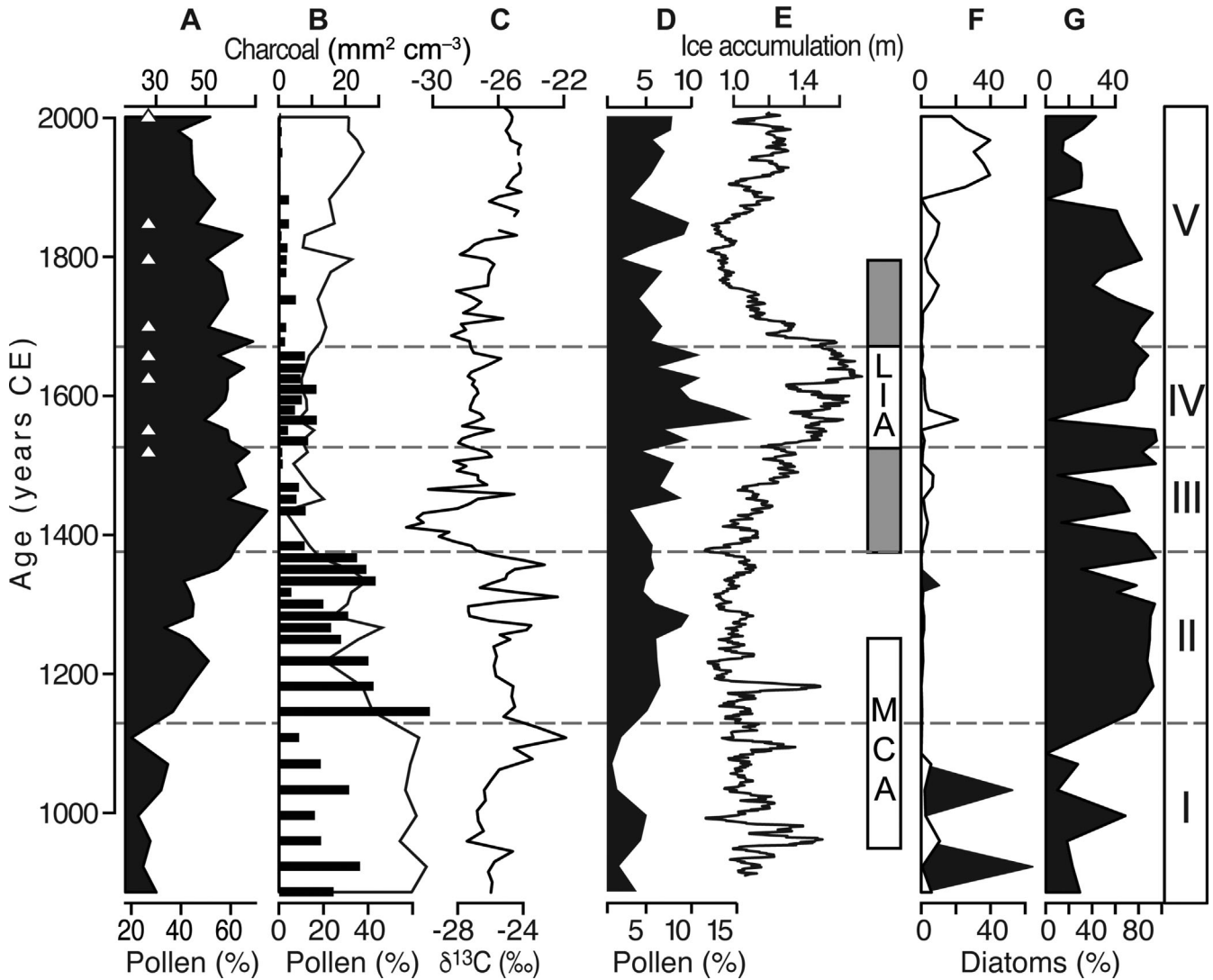


Figure 4. Summary of the palaeoenvironmental proxies in the sediment sequence from Lake San Carlos, Panama. (A) Tropical rainforest pollen percentages, and presence of *Zea mays* (triangles). (B) Grasses and open vegetation pollen percentages (hollow silhouette), and charcoal concentrations (horizontal bars). (C) Carbon stable isotopes. (D) Lower montane forest pollen percentages. (E) Ice accumulation on the Quelccaya ice cap in Peru (Thompson *et al.*, 2013); chronological uncertainties associated with the Medieval Climate Anomaly (MCA) and the Little Ice Age (LIA) are shown in rectangles (LIA in white is derived from our age–depth model, with the grey rectangle showing where it would fall according to the alternative model). (F) Relative abundances of *Aulacoseira* spp. (black silhouette), and *Achnanthisium* spp. and *Nitzschia amphibia* (hollow silhouette). (G) Relative abundances of *Fragilaria crotonensis*.

age model implies uncertainties regarding the depths at which the LIA would reflect in our record (Fig. 2). Nevertheless, if we assumed the alternative age model, there would not be substantial changes in our interpretation, except for a more temporally constrained enrichment of the local flora with montane elements (Fig. 4).

The last 350 years have been marked by a progressive decrease in TRF and increases in relative abundance of grasses and $\delta^{13}\text{C}_{\text{org}}$ values. The presence of maize through this period indicates human disturbance, although charcoal concentrations at this time are the lowest of the record. It is possible that when human settlements became permanent, people suppressed fire after adopting more advanced agricultural technologies (Ellis *et al.*, 2013). From 2003 to 2014 CE, the maximum number of annual fires within a radius of 30 km around Lake San Carlos occurred in 2003 (24 events, Fig. 1). The area covers $\sim 2.6 \text{ km}^2$ around the lake and has an intermediate level of human occupation. Although the area represents 3.4% of the Panamanian territory, it accounts only for 2% of all fire events in Panama, indicating a possible anthropogenic suppression of fire activity. One additional element that suggests the changes of the last 350 years have

been strongly associated with human disturbance is the sudden increase and persistence of *Nitzschia amphibia* and *Achnanthisium* spp. in the diatom assemblage since ~ 1900 CE (Fig. 3), both genera commonly associated with cultural eutrophication characterized by high concentrations of phosphorus (Lange Bertalot, 2000; Bellinger *et al.*, 2006).

Main drivers of environmental change: abrupt and gradual changes

Although using standardized variables produced a less explicative ordination, we preferred it to the non-standardized ordination for two main reasons (Legendre and Legendre, 1998): (i) standardization takes all variables to the same units making comparable proxies with different scales of measurement (e.g. charcoal concentration, species relative abundance and $\delta^{13}\text{C}_{\text{org}}$); and (ii) standardization confers all variables the same ecological importance, an assumption more reasonable than considering relative abundance as a direct indication of the individual role in the ecosystem. The PCA ordination on standardized proxies clearly separated terrestrial from aquatic components of the record; whereas

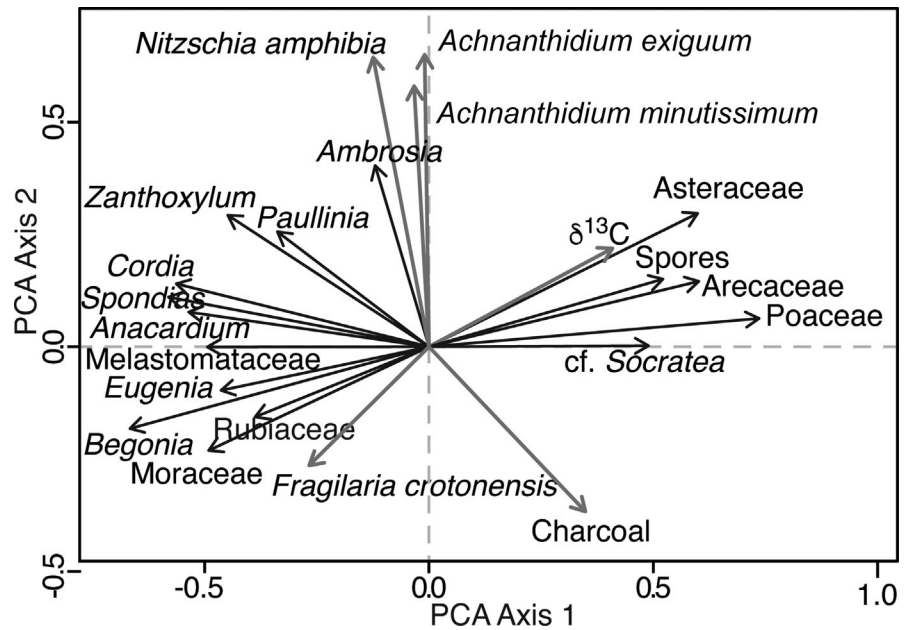


Figure 5. Correlation biplot of principal component analysis run using all variables from Lake San Carlos, Panama.

pollen taxa mostly aligned with PCA Axis 1, diatoms aligned with PCA Axis 2 (Fig. 5). Thus, the aquatic and terrestrial ecosystems, although probably driven by similar exogenic factors, showed independent responses. Such independence probably reflects the different temporal scales at which environmental drivers act upon terrestrial and aquatic ecosystems.

According to ecological preferences, Axis 1 had a clear direct relationship with soil moisture deficit. TRF taxa aligned on the negative side of Axis 1, whereas grasses and palm trees, usually associated with dry and/or seasonal conditions (Bush, 2000; Correa-Metrio *et al.*, 2011), displayed positive scores along this axis. Contrastingly, Axis 2 scores were directly associated with lake trophic status, with the separation of *F. crotonensis* from the other taxa suggesting slight variations in nutrient and light availability via this axis (Bradbury, 1988; St-Jacques *et al.*, 2009). Negative Axis 2 scores were associated with a low-light, slightly stratified mesotrophic lake, and positive scores were associated with a poorly mixed eutrophic lake. Thus, we interpret PCA Axis 1 as representative of vegetation variability (regional climate), and Axis 2 as representative of variability in the aquatic system (local conditions).

From the bottom of the record to ~1400 CE, high PCA Axis 1 scores support our initial interpretation of a climate system more seasonal than modern (Fig. 6). High erosion probably caused by precipitation has been reported for the Ecuadorian Andes (Moy *et al.*, 2002) and Galapagos Islands (Conroy *et al.*, 2008). Together with the San Carlos record, these lines of evidence suggest an invigorated activity of El Niño through this period. Nevertheless, evidence from corals that lie within the epicentre of El Niño–Southern Oscillation (ENSO) activity do not support this interpretation (Cobb *et al.*, 2013). Tree-ring reconstructions and climate models show pervasive droughts in western North America during the MCA (e.g. Cook *et al.*, 2010; Woodhouse *et al.*, 2010), conditions that have been linked to higher temperatures through this period (Woodhouse *et al.*, 2010). It is possible that the warmer global climate caused El Niño-like conditions expressed through high precipitation seasonality in Panama, intense rains in the Ecuadorian Andes and Galapagos Islands, and droughts in North America.

Moving probability density functions applied to the PCA scores were consistent with our initial interpretation. A first

abrupt change in both regional and local conditions (PCA axes 1 and 2) took place at ~1150 CE and was characterized by a substantial seasonality decrease, which caused increases in TRF taxa and a substantial turnover of diatom species (Figs. 4 and 6). This abrupt change was characterized by increasing variance and multimodal behaviour of the system (Fig. 6), suggesting the existence of a tipping point (*sensu* Lenton, 2011), which could have been the result of passing a critical threshold associated with the decreasing sea surface temperatures reported for the Panamanian Pacific (Toth *et al.*, 2015). A second abrupt change in regional conditions (PCA Axis 1) occurred at ~1350 CE (Figs. 4 and 6), marking the transition towards an even less seasonal distribution of precipitation throughout the year and the establishment of a TRF, and coinciding with decreasing erosion in the Andes and Galapagos Islands (Moy *et al.*, 2002; Conroy *et al.*, 2008).

From 1600 CE to the present, changes were rather gradual, although increases of variance in both PCA axes suggest larger environmental variability (Fig. 6). After the abrupt change of Axis 1 at ~1350 CE, the signal of PCA Axis 2 shows a substantial variance increase, and the average signal is closely associated with total solar irradiance (Moy *et al.*, 2002). High (low) solar irradiance is associated with high (intermediate) lake trophic state conditions. Similar to the Yucatán Peninsula (Hodell *et al.*, 2001), high solar irradiance may be associated with relatively dry episodes, which would result in greater evaporation and consequent lake eutrophication. It is likely that the insolation signal was always present in the lake component, but until ~1600 CE was overridden by the more powerful effects of the high seasonality that characterized the region.

Overall, the most obvious changes in the terrestrial and aquatic ecosystems were very probably associated with seasonality changes, with the date ~1350 CE marking a clear transition towards a less seasonal climate. High abundances of small charcoal particles reveal the persistence of intense and frequent regional fires from ~950 to 1350 CE (Fig. 6). The modern association of fire frequency with El Niño events (Fig. 1) and high charcoal concentrations through the MCA offer evidence of an El Niño-like seasonality pattern through this period. Nevertheless, there were two stages within this high-seasonality time interval. From ~950 to ~1175 CE, the region was characterized by higher sea surface temperatures and the highest seasonality of the last millennium. This

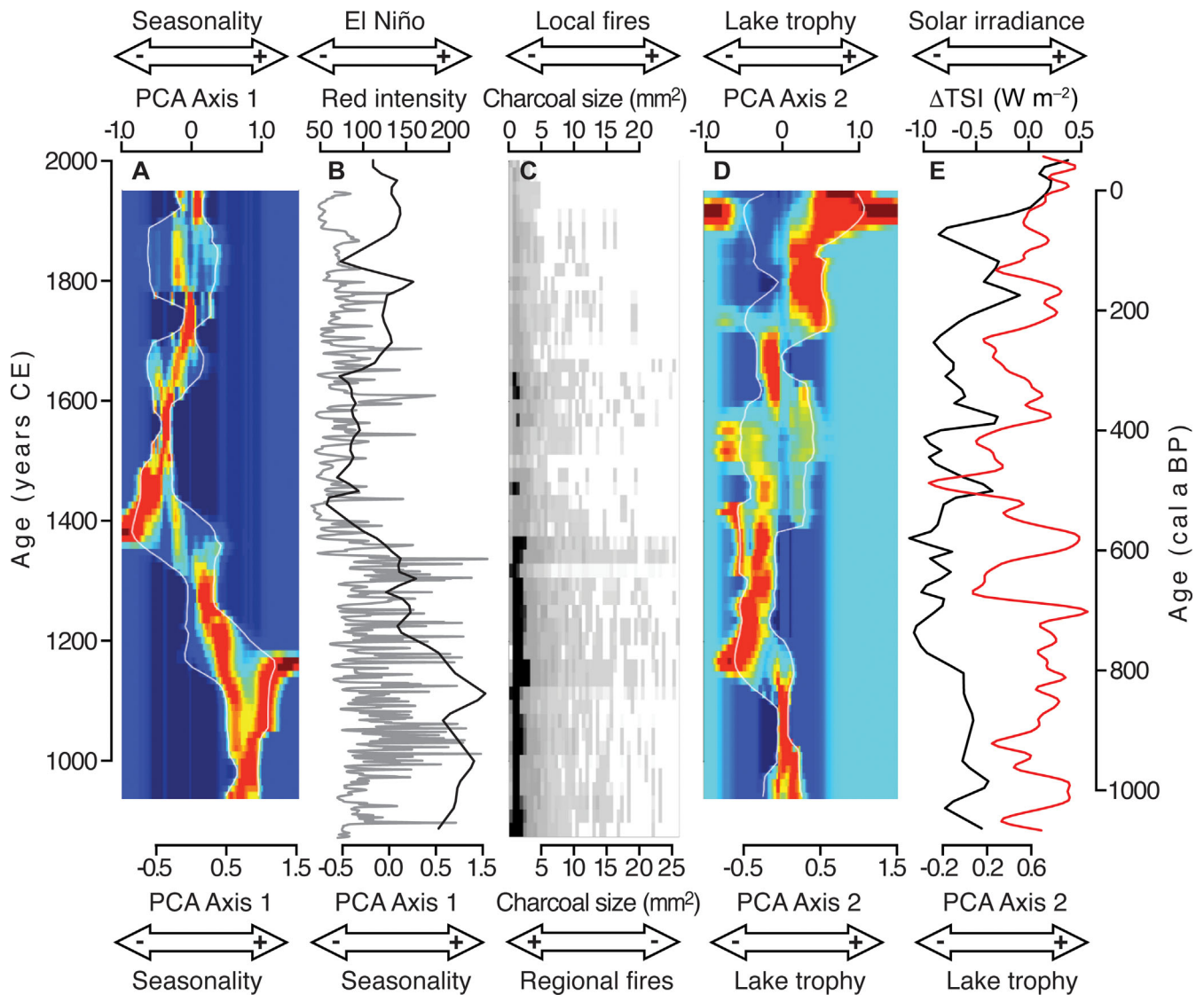


Figure 6. Environmental history of Lake San Carlos, Panama. (A) The running probability density function for PCA Axis 1, summarizing vegetation variability through time; from deep blue to red, the probability density increases, and the white lines represent the 95% confidence interval. (B) PCA Axis 1 sample scores (black line) overlain on El Niño activity (grey line) (Moy *et al.*, 2002). (C) Charcoal size classes; high abundances in black, absence in white. (D) The running probability density function over PCA Axis 2, summarizing lake trophic state variability through time; from deep blue to red, the probability density increases, and the white lines represent the 95% confidence interval. (E) PCA Axis 1 sample scores (black line), overlain on solar irradiance (red).

climate system abruptly transitioned to a second phase of less seasonality (from ~1150 to 1350 CE). From 1350 CE to the present, the system has been characterized by a relatively aseasonal precipitation regime, and the lake trophic state has been strongly influenced by insolation, possibly as an indirect result of changes in total annual precipitation.

The instability of the lake system during the last 600 years has probably been associated with local dynamics. Indeed, since 1550 CE, the presence of *Z. mays* in the San Carlos record is evidence for human occupation as an important local driver of the system. Additionally, a temperature decline (~1.8 °C) between ~1500 and ~1700 CE, which was not detected by the PCA, was identified from a substantial increase in montane taxa. This increase was coincident with maximum ice accumulation in the Andes (Thompson *et al.*, 2013), which probably resulted from wetter and relatively colder conditions in the Neotropics.

Conclusions

Our results show that during the last ~1100 years, aquatic and terrestrial ecosystem dynamics at middle elevations in

Panama were driven mostly by global climate variability. The dominance of highly seasonal forests in the region coincided with El Niño-like conditions reported for other regions (Moy *et al.*, 2002; Conroy *et al.*, 2008) and a warmer planet during the MCA (Mann *et al.*, 2009). Although predictions for ENSO behaviour in the coming century are poorly constrained, the IPCC foresees that ENSO-related precipitation variability will probably intensify within the next few decades (IPCC, 2013). Intensified precipitation variability, together with higher temperatures, will probably push the system towards conditions similar to those during the MCA. This will result in a change from TRF, which dominates the region today, to more open, deciduous vegetation. This scenario has important consequences in terms of biodiversity loss and release of carbon stored in soils and live biomass. Whereas the warmer conditions of the MCA were associated with a highly dynamic system and abrupt changes, cooling during the LIA was not associated with substantial changes in the vegetation or the lake. This highlights the fact that ecosystem responses to climate change are not linear, and that dramatic vegetation turnovers are probably associated with warming and changing seasonality.

The sediment record from Lake San Carlos illustrates that the terrestrial and aquatic ecosystems have been subject to high climate variability during the late Holocene, and as a consequence have been occupied by different biotic communities. Thus, environmental stability does not explain the high diversity in tropical piedmonts and middle elevations, as has been hypothesized (Sandel *et al.*, 2011). The record also shows that ecosystems are more dynamic and adaptable than commonly thought. The global temperature rise that is predicted for the next few centuries evidently does not represent a dire threat for biodiversity at middle elevations in the tropics. Indeed, populations in the region have adapted to abrupt changes in the past through equally abrupt responses (Correa-Metrio *et al.*, 2014). Such fast responses of communities have probably been facilitated by landscape heterogeneity, which enables disjunct populations to persist through times of environmental hardship (Bush, 2002). Thus, the most dangerous threat to biodiversity will come from climate change in the context of human-driven homogenization of the landscape and habitat fragmentation.

Acknowledgements. We thank the community of San Carlos for granting us access to the lake. We thank C. Jaramillo from Smithsonian Tropical Research Institute for facilitating field logistics. We are grateful to W. Gosling and two anonymous reviewers for constructive discussion on the original manuscript. Financial support came from the Inter-American Institute for Global Change Research (IAI, grant no. CRN3038), the US National Science Foundation (grant GEO-1128040), and the University of Regina start-up funds to M. Vézé.

Supplementary Information

Appendix S1. Photographs of lake San Carlos.

Appendix S2. Chronological control.

Appendix S3. Pollen diagram.

Appendix S4. Diatom diagram.

Abbreviations. ENSO, El Niño–Southern Oscillation; LIA, Little Ice Age; LMF, lower montane forest; MCA, Medieval Climate Anomaly; PCA, principal components analysis; TRF, tropical rainforest.

References

- Battarbee RW, Jones VJ, Flower RJ *et al.* 2001. Diatoms In *Tracking Environmental Change Using Lake Sediments: Terrestrial, Algal, and Siliceous Indicators*, Smol JP, Birks HJB, Last WM (eds). Kluwer Academic Publishers: Dordrecht; 155–202.
- Bellinger BJ, Cocquyt C, O'Reilly CM. 2006. Benthic diatoms as indicators of eutrophication in tropical streams. *Hydrobiologia* **573**: 75–87.
- Blaauw M, Christen JA. 2011. Flexible paleoclimate age–depth models using an autoregressive gamma process. *Bayesian Analysis* **6**: 457–474.
- Bradbury JP. 1988. A climatic-limnologic model of diatom succession for paleolimnological interpretation of varved sediments at Elk Lake, Minnesota. *Journal of Paleolimnology* **1**: 115–131.
- Bruijnzeel L. 2001. Hydrology of tropical montane cloud forests: a reassessment. *Land Use and Water Resources Research* **1**: 1–1.
- Bush MB. 2000. Deriving response matrices from Central American modern pollen rain. *Quaternary Research* **54**: 132–143.
- Bush MB. 2002. Distributional change and conservation on the Andean flank: a palaeoecological perspective. *Global Ecology and Biogeography* **11**: 463–467.
- Bush MB, Colinvaux PA. 1990. A pollen record of a complete glacial cycle from lowland Panama. *Journal of Vegetation Science* **1**: 105–119.
- Bush MB, Piperno DR, Colinvaux PA *et al.* 1992. A 14,300-year paleoecological profile of a lowland tropical lake in Panama. *Ecological Monographs* **62**: 251–276.
- Clark JS. 1988. Particle motion and the theory of charcoal analysis: source area, transport, deposition, and sampling. *Quaternary Research* **30**: 67–80.
- Cobb KM, Westphal N, Sayani HR *et al.* 2013. Highly variable El Niño–Southern Oscillation throughout the Holocene. *Science* **339**: 67–70.
- Colinvaux P, de Olivera PE, Moreno PJE. 1999. *Amazon Pollen Manual and Atlas*. Harwood Academic Publishers: Amsterdam.
- Conroy JL, Overpeck JT, Cole JE *et al.* 2008. Holocene changes in eastern tropical Pacific climate inferred from a Galápagos lake sediment record. *Quaternary Science Reviews* **27**: 1166–1180.
- Cook ER, Seager R, Heim RR *et al.* 2010. Megadroughts in North America: placing IPCC projections of hydroclimatic change in a long-term palaeoclimate context. *Journal of Quaternary Science* **25**: 48–61.
- Cooke R. 2005. Prehistory of Native Americans on the Central American Land Bridge: colonization, dispersal, and divergence. *Journal of Archaeological Research* **13**: 129–187.
- Correa-Metrio A, Bush MB, Pérez L *et al.* 2011. Pollen distribution along climatic and biogeographic gradients in northern Central America. *The Holocene* **21**: 681–692.
- Correa-Metrio A, Meave JA, Lozano-García S *et al.* 2014. Environmental determinism and neutrality in vegetation at millennial time scales. *Journal of Vegetation Science* **25**: 627–635.
- Ellis EC, Kaplan JO, Fuller DQ *et al.* 2013. Used planet: a global history. *Proceedings of the National Academy of Sciences of the United States of America* **110**: 7978–7985.
- Faegri K, Iversen J. 1989. *Textbook of Pollen Analysis*, 4th edn. Wiley: Chichester.
- Giglio L, Descloux J, Justice CO *et al.* 2003. An enhanced contextual fire detection algorithm for MODIS. *Remote Sensing of Environment* **87**: 273–282.
- Graham A. 2010. *Late Cretaceous and Cenozoic History of Latin American Vegetation and Terrestrial Environments*. Missouri Botanical Garden Press: St Louis.
- Haug GH, Günther D, Peterson LC *et al.* 2003. Climate and the collapse of Maya civilization. *Science* **299**: 1731–1734.
- Hodell DA, Brenner M, Curtis JH *et al.* 2001. Solar forcing of drought frequency in the Maya lowlands. *Science* **292**: 1367–1370.
- Hodell DA, Brenner M, Curtis JH *et al.* 2005. Climate change on the Yucatán Peninsula during the Little Ice Age. *Quaternary Research* **63**: 109–121.
- Holdridge LR, Mason FB, Hatheway WC. 1964. *Life Zone Ecology*. Centro Científico Tropical: San José, Costa Rica.
- IPCC. 2013 *Climate Change 2013: the Physical Science Basis*. Contribution of Working Group I to the Fifth Assessment Report of the Intergovernmental Panel on Climate Change. Cambridge University Press: Cambridge.
- Juggins S. 2007. C2, 1.5 ed, *Software for ecological and palaeoecological data analysis and visualisation*. Newcastle University: Newcastle upon Tyne.
- Lachniet MS, Burns SJ, Piperno DR *et al.* 2004. A 1500-year El Niño/Southern Oscillation and rainfall history for the Isthmus of Panama from speleothem calcite. *Journal of Geophysical Research* **109**: D20117.
- Lange Bertalot H. 2000. *Diatoms of the Andes from Venezuela to Patagonia/Tierra del Fuego*. Koeltz Scientific Books: Oberreifenberg, Germany.
- Legendre P, Legendre L. 1998. *Numerical Ecology*. Elsevier Scientific: Oxford.
- Leigh EG, O'Dea A, Vermeij GJ. 2014. Historical biogeography of the Isthmus of Panama. *Biological Reviews of the Cambridge Philosophical Society* **89**: 148–172.
- Lenton TM. 2011. Early warning of climate tipping points. *Nature Climate Change* **1**: 201–209.
- Loarie SR, Duffy PB, Hamilton H *et al.* 2009. The velocity of climate change. *Nature* **462**: 1052–1055.
- Lozano-García MS, Caballero-Miranda M, Ortega-Guerrero B *et al.* 2007. Tracing the effects of the Little Ice Age in the tropical lowlands of eastern Mesoamerica. *Proceedings of the National Academy of Sciences of the United States of America* **104**: 16200–16203.

- Mann ME, Zhang Z, Rutherford S *et al.* 2009. Global signatures and dynamical origins of the Little Ice Age and Medieval Climate Anomaly. *Science* **326**: 1256–1260.
- Marchant R, Almeida L, Behling H *et al.* 2002. Distribution and ecology of parent taxa of pollen lodged within the Latin American Pollen Database. *Review of Palaeobotany and Palynology* **121**: 1–75.
- Meyers PA. 2003. Applications of organic geochemistry to paleolimnological reconstructions: a summary of examples from the Laurentian Great Lakes. *Organic Geochemistry* **34**: 261–289.
- Moy CM, Seltzer GO, Rodbell DT *et al.* 2002. Variability of El Niño/Southern Oscillation activity at millennial timescales during the Holocene epoch. *Nature* **420**: 162–165.
- Novello VF, Cruz FW, Karmann I *et al.* 2012. Multidecadal climate variability in Brazil's Nordeste during the last 3000 years based on speleothem isotope records. *Geophysical Research Letters* **39**: L23706.
- Piperno DR. 2006. Quaternary environmental history and agricultural impact on vegetation in Central America. *Annals of the Missouri Botanical Garden* **93**: 274–293.
- Piperno DR, McMichael C, Bush MB. 2015. Amazonia and the Anthropocene: what was the spatial extent and intensity of human landscape modification in the Amazon Basin at the end of prehistory? *The Holocene* **25**: 1588–1597.
- R Core Team. 2015. *R: A Language and Environment for Statistical Computing*. R Foundation for Statistical Computing: Vienna.
- Reimer P, Bard E, Bayliss A *et al.* 2013. IntCal13 and Marine13 radiocarbon age calibration curves 0–50,000 years cal BP. *Radio-carbon* **55**: 1869–1887.
- Rodgers JC, Horn SP. 1996. Modern pollen spectra from Costa Rica. *Palaeogeography Palaeoclimatology Palaeoecology* **124**: 53–71.
- Sandel B, Arge L, Dalsgaard B *et al.* 2011. The influence of Late Quaternary climate-change velocity on species endemism. *Science* **334**: 660–664.
- Silverman BW. 1986. *Density Estimation for Statistics and Data Analysis*. Chapman & Hall: London.
- St-Jacques J.-M, Cumming BF, Smol JP. 2009. A 900-yr diatom and chrysophyte record of spring mixing and summer stratification from varved Lake Mina, west-central Minnesota, USA. *The Holocene* **19**: 537–547.
- Thompson LG, Mosley-Thompson E, Davis ME *et al.* 2013. Annually resolved ice core records of tropical climate variability over the past ~1800 years. *Science* **340**: 945–950.
- Toth LT, Aronson RB, Cobb KM *et al.* 2015. Climatic and biotic thresholds of coral-reef shutdown. *Nature Climate Change* **5**: 369–374.
- Woodhouse CA, Meko DM, MacDonald GM *et al.* 2010. A 1,200-year perspective of 21st century drought in southwestern North America. *Proceedings of the National Academy of Sciences USA* **107**: 21283–21288.